===

Dedicated to Full Member of the Russian Academy of Sciences
B.A. Trofimov on the 65th Anniversary of His Birth

Unexpected Reaction
of 2-Chloro-1-Phenylethane-1,1-dithiol with Hydrazine—
A New Route to 4,5-Dihydro-1,2,3-thiadiazoles

L. G. Shagun, V. A. Shagun, L. P. Ermolyuk, G. I. Sarapulova, and M. G. Voronkov

Favorskii Irkutsk Institute of Chemistry, Siberian Division, Russian Academy of Sciences,
ul. Favorskogo 1, Irkutsk, 664033 Russia
*e-mail: shagun@irioch.irk.ru*

Abstract—The reaction of 2-chloro-1-phenylethane-1,1-dithiol with hydrazine gave an unexpected product, 2-hydrazono-1-phenylethane-2,2-dithiol, which underwent intramolecular ring closure to 5-phenyl-4,5-dihydro-1,2,3-thiadiazole in 69% yield. Elementary steps of the process were studied by quantum-chemical methods, and their kinetic and thermodynamic parameters were determined.

While studying the chemical properties of 1-substituted 2-haloethane-1,1-dithiols, which were synthesized by us for the first time [1–3], we examined the reaction of 2-chloro-1-phenylethane-1,1-dithiol (**I**) with hydrazine. In keeping with the classical views on reactions of hydrazine with organic halogen compounds [4, 5], we expected that its reaction with halodithiol **I** will lead to 5-phenyl-1,2,3-thiadiazolidine through intermediate formation of 2-hydrazino-1-phenylethane-1,1-dithiol. Contrary to the expectations, compound **I** reacted with an alcoholic solution of hydrazine in anhydrous diethyl ether to give 2-hydrazono-1-phenylethane-1,1-dithiol (**II**) which underwent

intramolecular cyclization to 5-phenyl-4,5-dihydro-1,2,3-thiadiazole (**III**) (Scheme 1). An analogous pattern was observed [6] in the reaction of bromoacetophenone with hydrazine [6] (Scheme 2).

Quantum-chemical study of elementary steps of the reaction of **I** with hydrazine suggested a mechanism shown in Scheme 3. The initial reaction step is likely to follow the classical scheme to give short-lived intermediate **A** (which was not reliably detected so far). Due to its stereoelectronic properties, this intermediate almost instantaneously reacts with hydrazine with formation of a relatively stable (long-lived) intermediate **II**. Prototropic rearrangement of the latter

Scheme 1.

Scheme 2.

$$PhCOCH_2Br + 3NH_2NH_2 \longrightarrow PhCOCH{=}NNH_2 + N_2H_4 \cdot HBr + 2NH_3$$
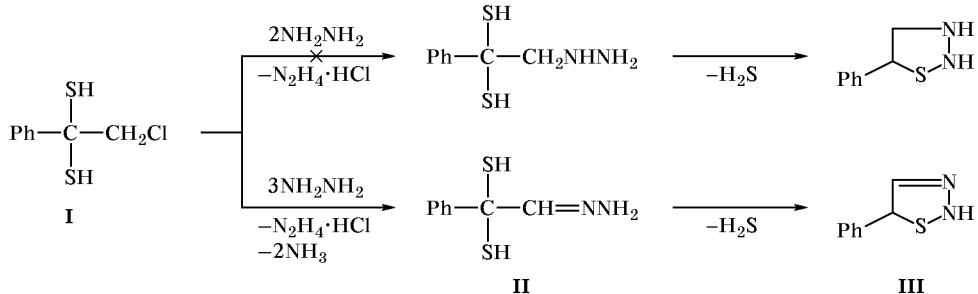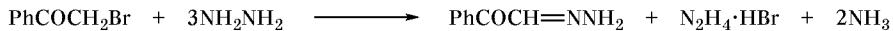
with elimination of hydrogen sulfide yields stable cyclic structure **III**. Quantum-chemical simulation of the main steps in Scheme 3 allowed us to elucidate factors responsible for the low stability of intermediate **A** and enhanced stability of acyclic hydrazone **II**, as well as to estimate the role of the geminal dithiol moiety in the dynamics of the transformation of **I** into **III**.

Scheme 3.

$$I \xrightarrow[-N_2H_4 \cdot HCl]{3NH_2NH_2} Ph-\underset{\underset{SH}{|}}{\overset{\overset{SH}{|}}{C}}-CH_2NHNH_2 \ + \ N_2H_4$$

A

$$\xrightarrow{-2NH_3} II \xrightarrow{-H_2S} III$$
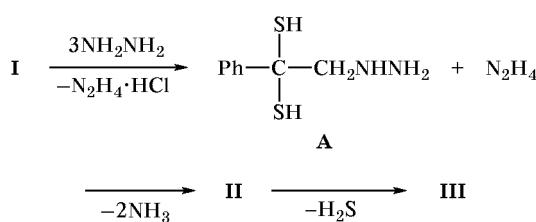
Nonempirical quantum-chemical calculations were performed in terms of the restricted Hartree–Fock approximation (RHF) [7, 8] with the 6-31G** valence-split basis set; GAUSSIAN-98 software was used [9]. The geometric parameters of molecular systems corresponding to transition structures ($\lambda = 1$, where λ is the number of negative Hessian eigenvalues for a given stationary point [10]) and energy minima ($\lambda = 0$) on the potential energy surface (PES) were optimized up to a gradient value of 10^{-5} a.u./bohr. While analyzing

planar PES regions, the limiting gradient value was set at 10^{-6} a.u./bohr. The force constant matrix was calculated using a subprogram incorporated in the GAUSSIAN software. Structures corresponding to energy minima on the PES were identified by moving along the gradient line (fastest descend technique) from the saddle point to the nearest critical point. For this purpose, a small initial shift along the transition vector was set, which allowed us to properly determine the reaction path [10].

The PES for rotational transformations of isolated molecule **I** suggests the existence of three spectroscopically distinguishable stationary states; their mutual transformations are characterized by an energy of activation exceeding 25 kJ/mol (Fig. 1). It was surprising that the least polar state **Ic** with opposite orientations of the electronegative sulfur and chlorine dipoles turned out to be the least stable. Presumably, positive interaction between the chlorine atom and thiol groups in structures **Ia** and **Ib** is stronger than the negative dipole–dipole interactions. No effect on the calculation results (within 3 kJ/mol; see table) was observed when a correction for zero-point vibration energy was introduced. The most polar structure **Ib** is a rotamer capable of forming with hydrazine the most stable prereaction bimolecular complex (Fig. 2, structure **IVa**). The stabilization energy of this complex is 144.9 kJ/mol (relative to the isolated

Total energies (E_{tot}, a.u.),[a] relative energies (ΔE, kJ/mol), numbers of negative Hessian eigenvalues (λ), zero-point harmonic vibration energies (ZPE, a.u.), imaginary of least harmonic frequencies (iw/w_1, cm^{-1}), and electric dipole moments (μ, D) of structures **I–V**, intermediate **A**, and transition states TS$_1$ and TS$_2$, according to the HF/6-31G** calculations

Structure	E_{tot}	ΔE	λ	ZPE	iw/w_1	μ
Ia	−1562.69091	0	0	0.15778	53	1.94
Ib	−1562.68125	25.3	0	0.15688	63	4.87
Ic	−1562.66024	85.5	0	0.15674	108	1.38
A	−1213.80826	–	0	0.20444	17	1.41
IIa	−1212.63601	0	0	0.17924	44	4.23
IIb	−1212.63150	11.8	0	0.17856	47	4.15
IIIa	−813.95988	18.9	0	0.15867	40	2.74
IIIb	−813.94840	49.0	0	0.15883	49	2.27
IIIc	−813.96710	0	0	0.15810	38	3.93
IVa	−1673.87121	0	0	0.21576	15	7.17
IVb	−1673.87176	−1.4	0	0.21608	19	5.94
TS$_1$	−1673.80492	173.9	1	0.21796	i481	10.46
Va	−1324.97328	0	0	0.26170	18	3.30
Vb	−1325.03980	−174.5	0	0.25794	20	3.29
TS$_2$	−1324.92512	126.3	1	0.25467	i238	6.67

[a] 1 a.u. = 2622.9897 kJ/mol.

fragments (with no ZPE taken into account; see table). Conformers **Ia** and **Ic** with hydrazine molecule form less stable complexes, by 9.7 and 17.7 kJ/mol, respectively. Complex **IVa** can be converted into bimolecular complex **IVb** through transition state TS_1 (energy of activation 173.9 kJ/mol; Fig. 2). In this step, the main contribution to the reaction coordinate is that of dissociation of the C–Cl bond. The degree of pyramidality of the nitrogen atom which attacks the carbocationic center strongly increases. The polarity of TS_1 increases to $\mu = 10.46$ D, and charge separation occurs in such a way that the positive charge appears to be delocalized more strongly than the negative charge. We can presume that increase in the solvent polarity and its electrophilicity should lead not only to greater initial population of the prereaction complexes but also to acceleration of the given step. The heat of the reaction is not large and is 1.4 kJ/mol. The energy of formation of complex **IVb**, 14.8 kJ/mol (relative to the particular components), is considerably lower than the energy of formation of complex **IVa**. This means that the lifetime of prereaction complex **IVa** should be considerably longer than the lifetime of **IVb**. Hydrogen chloride liberated during the process readily reacts with excess hydrazine and precipitates as hydrazine hydrochloride.

Intermediate **A** is characterized by a large number of possible rotational stationary states, the most stable of these being shown in Fig. 3. The reaction of intermediate **A** with hydrazine molecule to give complex **Va** (Fig. 3) is accompanied by conformational reorganization. As a result, its skeleton adopts a planar structure which is additionally stabilized by NH⋯S interactions. Such structural reorganization becomes possible due to reduced charge separation (and hence reduced negative dipole–dipole interactions) in the intermediate. Prereaction complex **Va** is more stable than its isolated components by 79.6 kJ/mol. It can be converted (through transition state TS_2) with an energy of activation of 126.3 kJ/mol into thermodynamically more stable complex **Vb** (Fig. 3; $\Delta H = 174.5$ kJ/mol). Stereoelectronic transformation of **Va** along the reaction coordinate occurs as follows. Interaction of lone electron pair on the nitrogen atom with one of the CH_2 protons leads to partial dissociation of the N–N bond in hydrazine molecule and increase in the N–C bond order via interaction of lone electron pair on the low-pyramidality nitrogen atom with the released carbon π-orbital. When the formation of π-bond is complete, the nitrogen atom becomes quaternized, and it donates proton to the partner, thus finishing dissociation of the hydrazine N–N bond and forming two ammonia molecules. The short life-
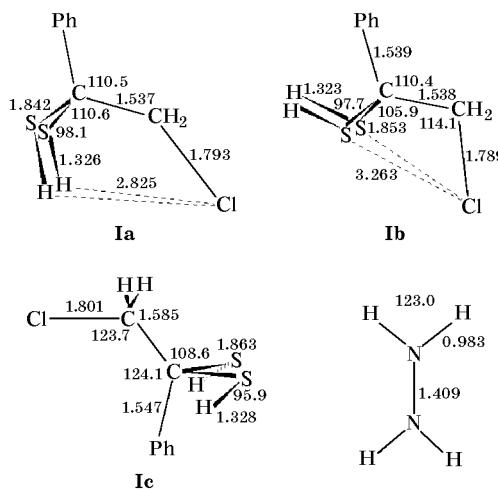
Fig. 1. Structures and geometric parameters (bond lengths, Å, and bond angles, deg) of the main stationary states of isolated molecules of compound **I** and hydrazine, calculated *ab initio* (RHF/6-31G**).
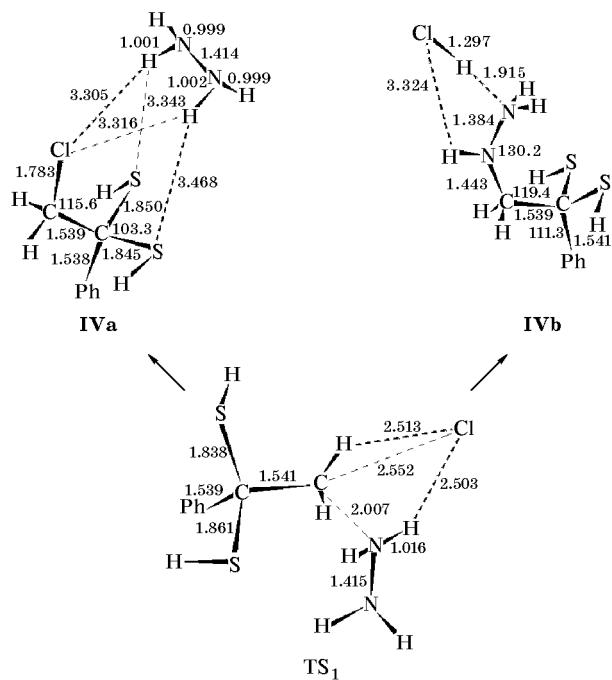
Fig. 2. Structures and geometric parameters (bond lengths, Å, and bond angles, deg) of bimolecular complexes **IVa** and **IVb** and the respective transition state TS_1, calculated *ab initio* (RHF/6-31G**).

time of intermediate **A** (which makes its preparative isolation impossible) can be interpreted in terms of a high probability for formation of exothermic prereaction complex **Va** and low barrier to its transformation into **Vb**. Taking into account a considerably higher degree of charge separation in TS_2 as compared
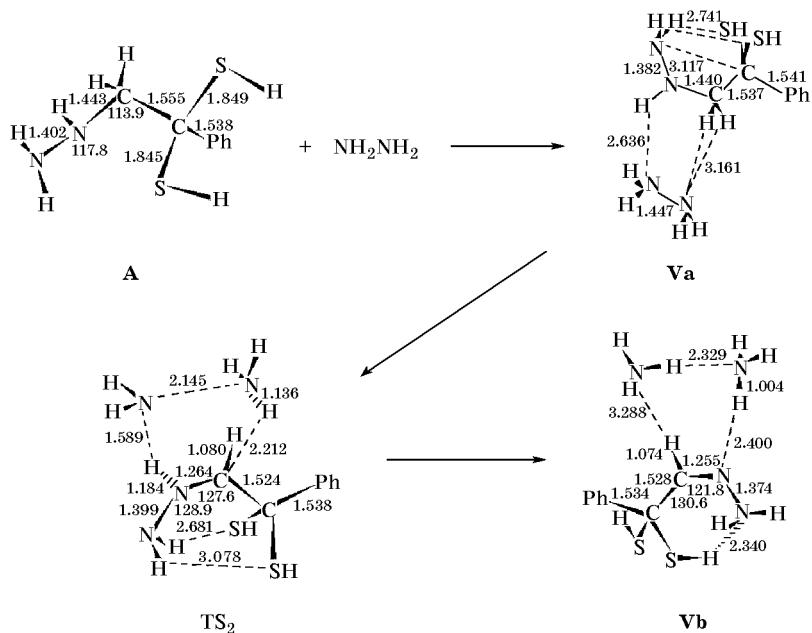
Fig. 3. Structures and geometric parameters (bond lengths, Å, and bond angles, deg) of intermediate **A**, bimolecular complexes **Va** and **Vb**, and the respective transition state TS_2, calculated *ab initio* (RHF/6-31G**).
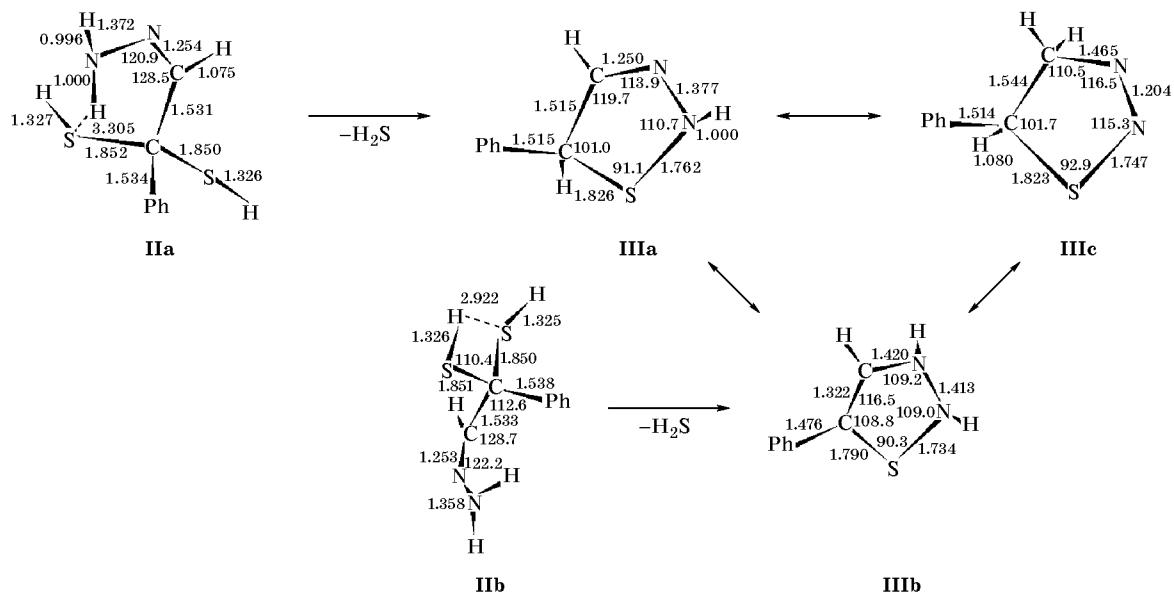
Fig. 4. Molecular structures and geometric parameters (bond lengths, Å, and bond angles, deg) of acyclic (**IIa**, **IIb**) and cyclic (**IIIa–IIIc**) compounds, calculated *ab initio* (RHF/6-31G**).

to **Va**, it is natural to expect that in polar medium the energy of activation should be even lower.

Isolated molecule of hydrazone **II** can also exist as different rotamers. The most stable are structures **IIa** and **IIb** (Fig. 4); the activation barrier to their inter-conversion exceeds 25 kJ/mol. These structures lose hydrogen sulfide with time, yielding tautomers **IIIa**–

IIIc (Fig. 4). Analysis of the potential energy surface for the cyclization process suggests several possible mechanisms. According to the calculations, tautomer **IIIa** is formed via a channel involving 1,5-shift of the imino group proton to the thiol group, dissociation of the C–S bond, 1,2-shift of the thiol proton to the carbanionic center, and cyclization via C–N bond

closure (Scheme 4). The rate-determining stage in this sequence is the 1,5-prototropic shift; its energy of activation is 189.4 kJ/mol.

Scheme 4.
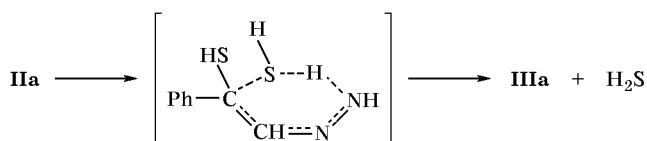
Another reaction channel leading to cyclic structure **IIIb** includes intramolecular autoprotonation and elimination of hydrogen sulfide in the limiting stage (Scheme 5).

Scheme 5.
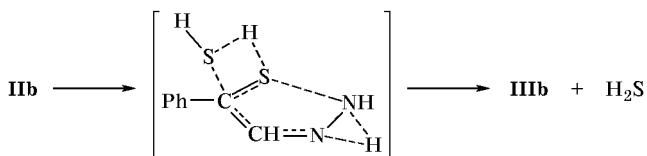
Its energy of activation is 273.6 kJ/mol. As shown in [11], the barrier can be reduced to an appreciable extent when some mediator molecules participate in the autoprotonation process. The formation and accumulation of cyclic structure **IIIc** are most likely to result from the intramolecular prototropic rearrangement **IIIa → IIIc**, which is characterized by an energy of activation of 239.4 kJ/mol. We failed to find a direct gradient path with a comparable energy of activation by considering several schemes for elementary steps of the transformation **II → IIIc** + H_2S. Structure **IIIc** is the most stable from the viewpoint of thermodynamics; it is superior in stability to structures **IIIa** (by 18.9 kJ/mol) and **IIIb** (by 49.0 kJ/mol). These results remain almost unchanged (within 2–3 kJ/mol) when a correction for ZPE is taken into account.

EXPERIMENTAL

The IR spectra were recorded on a Specord 75IR instrument from solutions in $CDCl_3$. The ^{1}H and ^{13}C NMR spectra were obtained on a Bruker DPX-400 spectrometer using $CDCl_3$ as solvent and HMDS as internal reference. The progress of reactions was monitored by TLC on Silufol UV-254 plates with chloroform as eluent.

5-Phenyl-4,5-dihydro-1,2,3-thiadiazole (III). A cold (–50°C) solution of 0.1 g (3 mmol) of hydra-zine in 2 ml of anhydrous diethyl ether was gradually added to a solution of 0.2 g (1 mmol) of dithiol **I** in 10 ml of anhydrous diethyl ether, cooled to –50°C. The mixture was kept at that temperature, the precipitate was filtered off, and the filtrate was evaporated under reduced pressure. The yellow oily residue was dissolved in 3 ml of chloroform, and 10 ml of hexane was added. The precipitate was filtered off and dried under reduced pressure. Yield 0.11 g (69%), light yellow powder, mp 73–74°C. IR spectrum, ν, cm^{-1}: 3300 (NH); 1630 (C=N); 1590, 1570, 1480, 1270 (Ph). ^{1}H NMR spectrum, δ, ppm: 3.85 d (1H, PHC**H**), 4.14 s (1H, HC=N), 7.45 m (5H, H_{arom}), 8.5 s (1H, NH). ^{13}C NMR spectrum, $δ_C$, ppm: 45 (**C**Ph), 127–133 (C_{arom}), 195 (C=N). Found, %: C 58.02; H 5.28; N 16.40; S 19.69. $C_8H_8N_2S$. Calculated, %: C 58.53; H 4.87; N 17.07; S 19.51.

IR monitoring of the reaction of compound I with hydrazine. A small part of the reaction mixture prepared for the synthesis of **III** was cooled to –50°C and placed in a spectrophotometric cell cooled to –50°C. The spectrum of the mixture displayed appearance of new absorption bands (1500, 1630, 1670, 3300 cm^{-1}) due to formation of acyclic hydrazone structure **II** and (partially) of cyclic product **III**. With time, the absorption intensity at 1670 cm^{-1} (compound **II**) [11] quickly fell down, while the intensity of the absorption band at 1630 cm^{-1} (product **III**) [12] sharply increased.

REFERENCES

1. Shagun, L.G., Usova, T.L., Voronkov, M.G., Usov, V.A., Romanenko, L.S., and Efremova, G.G., *Zh. Org. Khim.,* 1990, vol. 26, p. 2029.

2. Shagun, L.G., Papernaya, L.K., Voronkov, M.G., Dabizha, O.N., Sarapulova, G.I., and Timokhina, L.V., *Russ. J. Org. Chem.,* 1999, vol. 35, p. 354.

3. Shagun, L.G., Dorofeev, I.A., Ermolyuk, L.P., Sarapulova, G.I., and Voronkov, M.G., *Russ. J. Org. Chem.,* 2001, vol. 37, p. 1207.

4. Grekov, A.P., *Organicheskaya khimiya gidrazina* (Organic Chemistry of Hydrazine), Kiev: Tekhnika, 1966, p. 66.

5. Potekhin, B.V., Kuznetsov, M.A., and Potekhin, A.A., *Khimiya organicheskikh proizvodnykh gidrazina* (Chemistry of Organic Hydrazine Derivatives), Leningrad: Khimiya, 1979, p. 223.

6. Hauptmann, S., Klude, M., Seding, K.-D., and Wilde, H., *Angew. Chem.,* 1965, vol. 77, p. 678.

7. Minkin, V.I., Simkin, B.Yu., and Minyaev, R.M., *Quantum Chemistry of Organic Compounds. Mechanisms of Reactions,* Berlin: Springer, 1990, p. 277.

8. Herhe, V.J., Radom, L., Schleyer, P.V.R., and Pople, J.A., *Ab Initio Molecular Orbital Theory,* New York: Wiley, 1986, p. 300.

9. Frisch, M.J., Trucks, G.W., Schlegel, H.B., Scuseria, G.E., Robb, M.A., Cheeseman, J.R., Zakrzewski, V.G., Montgomery, J.A., Stratmann, R.E., Burant, J.C., Dapprich, S., Millam, J.M., Daniels, A.D., Kudim, K.N., Strain, M.C., Farkas, O., Tomasi, J., Barone, V., Cossi, M., Mennucci, B., Pomelli, C., Adamo, C., Clifford, S., Ochterski, J., Petersson, G.A., Ayala, P.Y., Cui, Q., Morokuma, K., Malick, D.K., Rabuck, A.D., Raghavachari, K., Foresman, J.B., Cioslowski, J., Ortiz, J.V., Stefanov, B.B., Liu, G., Liashenko, A., Piskorz, P., Komaromi, I., Comperts, R., Martin, R.L., Fox, D.J., Keith, T., Al-Laham, M.A., Peng, C.Y., Nanayakkara, A., Gonzalez, C., Challacombe, M., Gill, P.M.W., Johnson, B., Chen, W., Wong, M.W., Andres, J.L., Gonzalez, C., Head-Gordon, M., Replogle, E.S., and Pople, J.A., *GAUSSIAN 98, Revision A.6,* Pittsburgh, PA: Gaussian, 1998.

10. Minyaev, R.M., *Usp. Khim.,* 1994, vol. 63, p. 939.

11. Kuznetsov, V.V., *Russ. J. Org. Chem.,* 1999, vol. 35, p. 1713.

12. *Physical Methods in Heterocyclic Chemistry,* Katritzky, A.R., Ed., New York: Academic, 1963. Translated under the title *Fizicheskie metody v khimii geterotsiklicheskikh soedinenii,* Moscow: Khimiya, 1966, p. 660.